Influence of Template/Functional Monomer/Cross-Linking Monomer Ratio on Particle Size and Binding Properties of Molecularly Imprinted Nanoparticles

Keiichi Yoshimatsu,[1] Tomohiko Yamazaki,[2] Ioannis S. Chronakis,[3] Lei Ye[1]

[1]*Pure and Applied Biochemistry, Chemical Center, Lund University, S-221 00 Lund, Sweden*
[2]*International Center for Materials Nanoarchitectonics (MANA) and Biomaterials center (BMC), National Institute for Materials Science (NIMS), 1-1 Namiki, Tsukuba, Ibaraki 305-0044, Japan*
[3]*Technical University of Denmark, DTU Food, B227, 2800 Kgs. Lyngby, Denmark*

Received 2 March 2011; accepted 22 June 2011
DOI 10.1002/app.35150
Published online 13 October 2011 in Wiley Online Library (wileyonlinelibrary.com).

ABSTRACT: A series of molecularly imprinted polymer nanoparticles have been synthesized employing various template/functional monomer/crosslinking monomer ratio and characterized in detail to elucidate the correlation between the synthetic conditions used and the properties (e.g., particle size and template binding properties) of the obtained nanoparticles. In brief, the presence of propranolol (template) in the polymerization mixture turned out to be a critical factor on determination of the size as well as the binding properties of the imprinted nanoparticles. The functional monomer/crosslinking monomer ratio significantly affects the binding capability of the imprinted nanoparticles, but its influence on the size of the nanoparticles was found to be rather limited. The results obtained provide valuable clues for designing molecularly imprinted nanoparticle preparation in future studies, where fine tuning of particle size and binding properties are required to fit practical applications. © 2011 Wiley Periodicals, Inc. J Appl Polym Sci 124: 1249–1255, 2012

Key words: molecular imprinting; polymer; nanoparticle; propranolol; precipitation polymerization

INTRODUCTION

Polymer particles with a physical size of a few nanometers to several micrometers are of great interest in a broad range of scientific fields including chemistry and materials science.[1–5] Particularly, nanoparticles and microspheres with selective molecular recognition properties are very attractive, because they can be easily incorporated into existing analytical or preparative platforms to solve various practical problems. Typically, functional particles with molecular recognition capability are prepared by immobilizing biological macromolecules such as antibodies onto supporting particles.[6–9] However, the poor stability and the expensive production cost of biological recognition materials are considered as serious drawbacks of this methodology. A promising alternative method is to create selective molecular recognition sites in the matrix of polymer particles directly by using molecular imprinting strategy.[10–14] In general, molecular imprinting strategy employs free-radical copolymerization of functional and crosslinking monomers in the presence of a "template" compound to create binding sites that have complementary shape and polarity against the template. After subsequent removal of the template, polymeric materials which contain selective molecular recognition sites can be obtained. Such highly crosslinked polymer materials can have a very high chemical and physical stability,[15] and thus molecularly imprinted polymers (MIPs) are attracting great attentions as a potential replacement of biological macromolecules to offer selective molecular recognition.[16–18]

With the traditional "bulk" polymerization method, MIPs are synthesized as a hard monolith, which must be ground into smaller particles for usage. This method is time-consuming, low-yield, and unsuitable for large scale preparation. More importantly, it can only provide irregularly shaped materials with a wide distribution of particle sizes, which are difficult to use in many practical applications. To overcome these limitations, we have previously reported a method for preparation of uniform MIP particles with diameters from a few hundred nanometers to several micrometers using precipitation polymerization.[19–21] Scheme 1 describes the schematic representation of the MIP particle synthesis method. The method involves polymerization of monomers in a near-θ solvent, where the formation of polymer particles takes place as a result of

Correspondence to: L. Ye (lei.ye@tbiokem.lth.se).
Contract grant sponsors: Swedish Research Council, Nanotechnology Innovation Center, National Institute of Materials Science (NIMS), Ministry of Education, Culture, Sports, Science and Technology (MEXT), Japan.

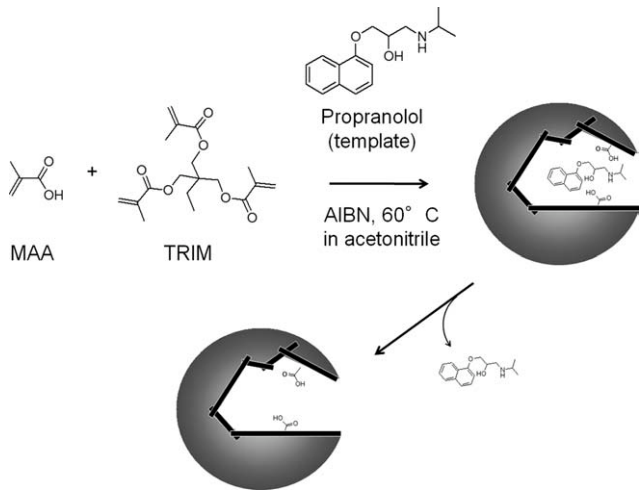

Scheme 1 Scheme of molecularly imprinted polymer nanoparticle synthesis.

entropic precipitation of nanogel particles and continuous capture of nascent oligomers.[22] Because no interfering reagent (i.e., surfactant or stabilizer) is required in this method, it is very easy to purify the synthesized MIP beads, and the method is generally applicable to a broad range of template structures.[23] Furthermore, taking advantage of their favorable physical forms, MIP beads synthesized using this method could be successfully applied in ligand binding assays,[19] solid-phase extraction,[24,25] liquid chromatography,[26] capillary electrochromatography,[27–29] and microfluidic extraction systems.[30] In addition, MIP nanoparticles synthesized by precipitation polymerization could be readily immobilized on the surface of a signal transducer to construct chemical sensors,[31,32] and be encapsulated into composite nanofibers to fabricate useful materials for chemical analysis.[33,34]

Despite the simplicity of the synthesis procedure, the mechanism of MIP particle formation is complex and remains not fully understood. As a consequence, the correlation between precipitation polymerization conditions and the properties of the resulting MIP particles requires further investigation. Previously, we have studied the influence of different crosslinkers on the physical and chemical properties of the resulting MIP beads.[20,21,35] However, the influences of other parameters, such as template/functional monomer/crosslinking monomer ratio etc., on particle size and binding properties of molecularly imprinted nanoparticles have not been critically investigated thus far. In this work, we investigate the influence of the ratio of template/functional monomer/crosslinking monomer on the properties of the resulting MIP nanoparticles. A series of nanoparticles are synthesized using different template/functional monomer/crosslinking monomer ratio, and their particle sizes and molecular binding properties are characterized in detail. The size of the nanoparticles was analyzed using scanning electron microscopy (SEM) and dynamic light scattering (DLS) measurements. Chemical composition of the nanopartiles was determined by elemental analysis, and the binding properties of the particles were studied through radioligand binding experiments. From the results obtained, we were able to identify several significant parameters in the preparation step that affect the properties of the resulting MIP nanoparticles.

EXPERIMENTAL

Materials

Trimethylolpropane trimethacrylate (TRIM, technical grade) were obtained from Aldrich (Dorset, UK). Acetic acid (glacial, 100%), acetonitrile (99.7%) and azobisisobutyronitrile (AIBN, 98%) used for polymer synthesis were purchased from Merck (Darmstadt, Germany). AIBN was recrystallized from methanol before use. Methacrylic acid (MAA, 98.5%) was purchased from ACROS (Geel, Belgium) and used as received. (*R*,*S*)-Propranolol hydrochloride (99%) supplied by Fluka (Dorset, UK) were converted into free base form before use. (*S*)-[4-^{3}H]-Propranolol (specific activity 555 GBq mmol^{-1}, 66.7 μ*M* solution in ethanol) was purchased from NEN Life Science Products Inc. (Boston, MA). Scintillation liquid, Ecoscint A was from National Diagnostics (Atlanta, GA). Other solvents were of analytical grade.

Apparatus

Dynamic light scattering measurement was performed on a DLS-6000 spectrophotometer (Otsuka Electronics, Osaka, Japan). Polymer particles (2 mg) were mixed with acetonitrile (1 mL) and sonicated in a benchtop ultrasonic cleaner for 20 min until no particle aggregate could be observed. The colloidal sample was diluted with 25 m*M* citrate buffer (pH 6.0):acetonitrile (50 : 50, v/v) to a final concentration of 20 μg mL^{-1} prior to particle size measurement. The hydrodynamic diameter of the particles was measured at 25°C. SEM imaging was carried out on a JSM-T300 scanning electron microscope (JEOL, Tokyo, Japan) unless otherwise stated. Polymer microspheres were sputter coated with gold prior to the SEM measurement. The carbon, hydrogen, and nitrogen content was determined using a vario MICRO cube elemental analyzer (Elementar Analysensysteme GmbH, Germany).

Polymer syntheses

Molecularly imprinted nanoparticles were synthesized using precipitation polymerization under the

TABLE I
Preparation of Polymer Nanoparticles

Polymer	MAA (wt %)	Propranolol (mg)	MAA (mg)	TRIM (mg)	C content[a] (wt %)	N content[a] (wt %)	$C_{50\%}$[b] (mg/mL)
MIP1	9	102	78	757	59.2	<0.3	1.3
NIP1	9	–	78	757	59.4	<0.3	–
MIP2	14	137	113	684	60.9	<0.3	0.7
NIP2	14	–	113	684	61	<0.3	–
MIP3	37	137	295	502	61.1	<0.3	–
NIP3	37	–	295	502	61.3	<0.3	–

[a] The values are determined by elemental analysis.
[b] The concentration of polymer particles that bound 50% of the radioligand.

conditions described in Table I. The template molecule, (*R*,*S*)-propranolol was dissolved in 40 mL of acetonitrile in a 150 mm × 25 mm borosilicate glass tube equipped with a screw cap. The functional monomer (MAA), the crosslinking monomer (TRIM) and the initiator (AIBN) were then added. The solution was purged with a gentle flow of N_2 for 5 min and sealed under N_2. Polymerization was carried out by inserting the borosilicate glass tube in a water bath preset to 60°C for 24 h. After polymerization, particles were collected by centrifugation. The template molecule and unreacted monomers were removed by batch mode solvent extraction with methanol containing 10% acetic acid (v/v), until no template could be detected from the washing solvent by UV-Vis spectrometric measurement. Polymer particles were finally washed with acetone and dried in a vacuum chamber.

Radio-ligand binding experiment

In a series of polypropylene microcentrifuge tubes, increasing amounts of polymer particles were suspended in a mixture of 25 m*M* citrate buffer (pH 6.0):acetonitrile (50 : 50, v/v). After addition of (*S*)-[4-^{3}H]-propranolol (246 fmol), the mixture was incubated at room temperature overnight. A rocking table was used to provide gentle mixing. After the incubation, samples were centrifuged at 14,000 rpm for 10 min. Supernatant (500 μL) was taken from each microcentrifuge tube and mixed with 10 mL of scintillation liquid (Ecoscint A), from which the radioactivity was measured using a model 1219 Rackbeta β-radiation counter from LKB Wallac (Sollentuna, Sweden). The amount of [^{3}H]-labeled propranolol bound to polymer particles was calculated by subtraction of the free fraction from the total amount added. Data are mean values of duplicate measurements.

Displacement experiment

In a series of polypropylene microcentrifuge tubes, a fixed amount of polymer particles and (*S*)-[4-^{3}H]-propranolol (246 fmol) were mixed in a mixture of 25 m*M* citrate buffer (pH 6.0):acetonitrile (50 : 50, v/v). To the tubes were added increasing amounts of nonlabeled (*R*)- and (*S*)-propranolol dissolved in the same solvent. Afterwards, the samples were incubated and processed in the same way as in the radio-ligand binding experiment.

RESULTS AND DISCUSSION

Preparation of nanoparticles

A precipitation polymerization method was employed for the synthesis of molecularly imprinted polymer (MIP) nanoparticles. Previously we reported the synthesis of MIP nanoparticles by free-radical copolymerization of methacrylic acid (MAA; a functional monomer) and trimethylolpropane trimethacrylate (TRIM; a crosslinking monomer) in acetonitrile, in the presence of a drug compound, propranolol acting as a model template.[19] In this study, we further investigate the synthesis of propranolol-imprinted nanoparticles using different ratios of template/functional monomer/crosslinking monomer. The total monomer concentration used in this study was ~ 2% (w/v) of the solvent. The percentage of MAA in the monomer mixture was varied from 9 wt %, 14 wt % to 37 wt % for MIP1, MIP2, and MIP3, respectively. A slightly excess amount of propranolol (template) relative to MAA (1–1.3 equivalents of MAA) was used for preparation of MIP1 and MIP2, following our previously reported protocol. For MIP3, the amount of propranolol used was the same as that for MIP2, resulting in a lower template/functional monomer ratio. This formulation was designed to assess the influence of functional monomer/crosslinking monomer straightforwardly. Nonimprinted control polymers, NIP1, NIP2, and NIP3 were synthesized under conditions identical to that used for synthesizing MIP1, MIP2, and MIP3, respectively, except for the omission of the template, (*R*,*S*)-propranolol.

Yield and elemental analysis of nanoparticles

The yields of polymer nanoparticles were higher than 95% for all the cases. The carbon and nitrogen

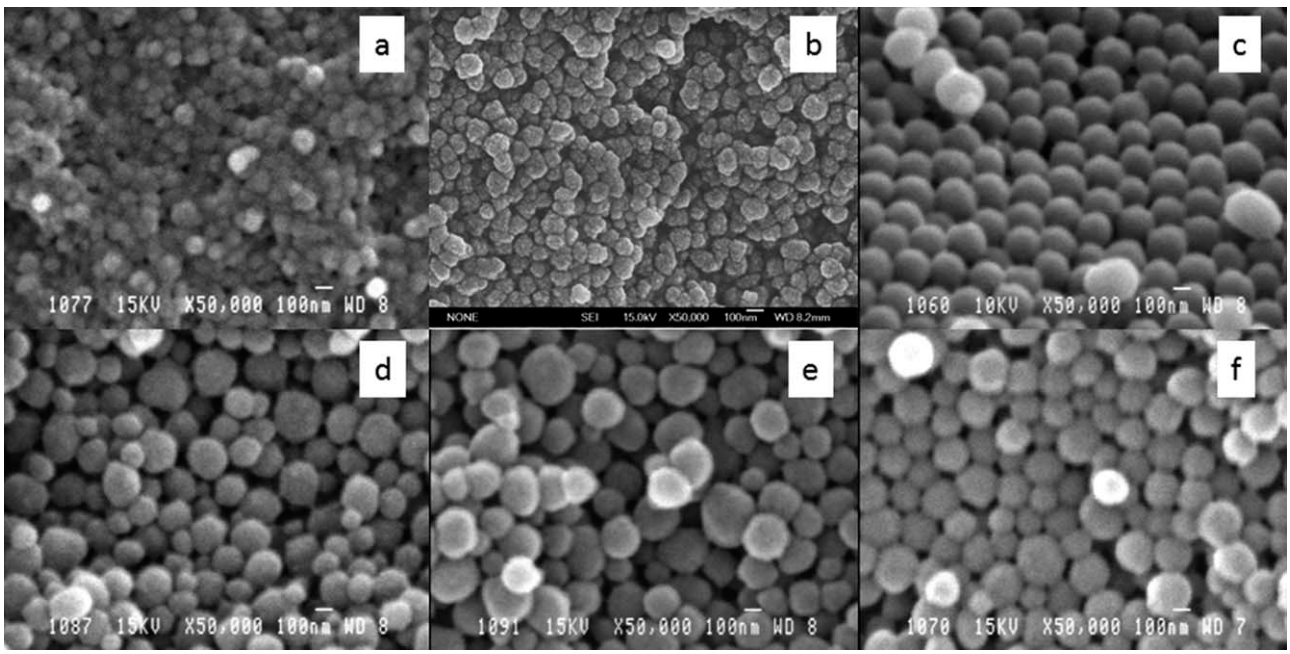

Figure 1 SEM microphotograph of nanoparticles. (a) MIP1: MAA 9 wt %, (b) MIP2: MAA 14 wt %, (c) MIP3: MAA 37 wt %, (d) NIP1: MAA 9 wt %, (e) NIP2: MAA 14 wt %, and (f) NIP3: MAA 37 wt %. All images were obtained with JEOL JSM-T300 microscope except for (b), which was obtained with JEOL JSM-6700F microscope.

content of nanoparticles were obtained by elemental microanalysis (Table I). The carbon content can be used to estimate the ratio of MAA and TRIM incorporated in the nanoparticles, because a TRIM monomer unit has a slightly higher carbon content than a MAA monomer unit. As shown in Table I, the measured carbon contents are in the order of MIP3 (NIP3) > MIP2 (NIP2) > MIP1 (NIP1). This result indicates that the MAA/TRIM ratio in the prepolymerization mixture is reflected by the actual ratio of MAA/TRIM incorporated in the solid particles, even though their correlation is not strictly linear. We should also point out that the elemental composition of the MIPs and their corresponding NIPs are almost identical, suggesting that the presence of the template does not influence the ratio of the incorporated monomers. The nitrogen content was determined to be <0.3% in all the polymers. This low nitrogen content may represent the incorporated initiator, and it indicates that most of propranolol template has been removed at the extraction step.

Particle size distribution of nanoparticles

From the SEM images, it is found that all the synthesized particles are spherical and are within the size range of several hundred nanometers (Fig. 1). To study the state of nanoparticles in solution, the particles were suspended in solvent and their hydrodynamic sizes were measured by DLS. As shown in Figure 2, it is clear that all the nanoparticles are monodispersed, and their hydrodynamic sizes are slightly larger than that can be estimated from the SEM images. The larger size value in solution can be attributed to particle swelling, which is in agreement with our previous findings. Furthermore, all the polymer nanoparticles have good colloidal stability in solution. This property is particularly favorable when one considers utilization of nanoparticles in binding assays and in microfluidic separation systems.[27–31]

To find out the factors that can most significantly influence the particle size, the average value of hydrodynamic diameters of the nanoparticles was plotted vs. the percentage of MAA used in the prepolymerization mixture (Fig. 3). While all the NIP nanoparticles are within the 400–450 nm range, the three types of MIP nanoparticles have significantly different sizes. The size of MIP1 and MIP2 are approximately [1/2]–[3/4] of the corresponding NIPs. It is interesting to notice that although particle size of MIP1 and MIP2 are somewhat different from their corresponding NIPs, the elemental compositions of them are found to be nearly identical. In the case of MIP3 and NIP3 (prepared using 37% MAA in the monomer mixture), the particle size of MIP3 is comparable with that of NIP3. These results lead to two important conclusions: (1) In a purely nonimprinting system, the amount of functional monomer (MAA) or the crosslinking density used has little effect on the hydrodynamic size of the synthesized poly(MAA-*co*-TRIM) nanoparticles. (2) The presence of template has a major effect on the size of the imprinted nanoparticles. However, this influence

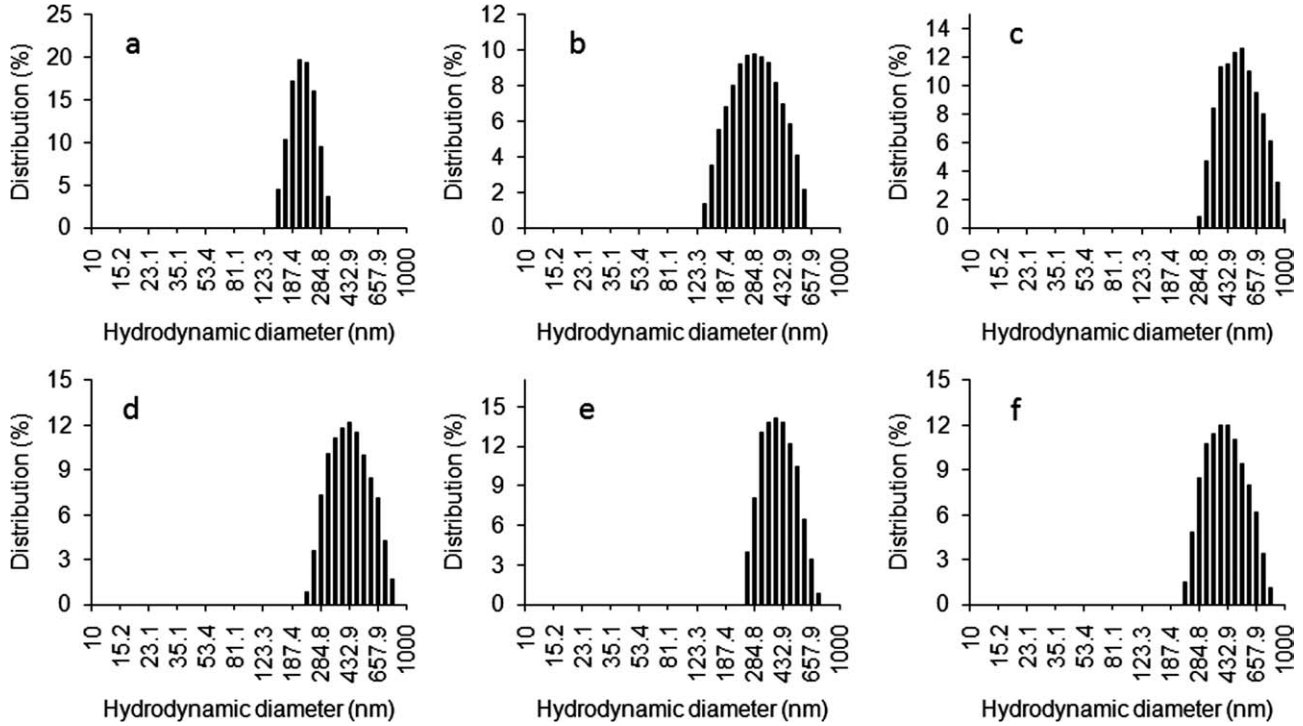

Figure 2 Particle size distribution of nanoparticles determined by dynamic light scattering (DLS). Measured in a mixture of 25 m*M* citrate buffer (pH 6):acetonitrile (1 : 1, v/v). (a) MIP1: MAA 9 wt %, (b) MIP2: MAA 14 wt %, (c) MIP3: MAA 37 wt %, (d) NIP1: MAA 9 wt %, (e) NIP2: MAA 14 wt % and (f) NIP3: MAA 37 wt %.

becomes less important at low crosslinking density when the ratio of propranolol/MAA is reduced. It seems that the particle size differences between MIPs and NIPs are presumably as a result of molecular interaction between MAA and propranolol. In fact, propranolol is an amphiphilic molecule composed of a hydrophobic naphthyl ring linked to a polar chain. It is possible that the interaction between propranolol and MAA (or the carboxyl group on the growing polymer chains) changes the solubility parameter of the growing polymer chains, thereby influences the particle growth processes.[36] A recent study in our group has shown that the presence of propranolol template affects also the rate of particle growth. On the other hand, when neutral and hydrophobic steroidal compounds are used as templates, the size of MIP nanoparticles becomes slightly larger than their corresponding NIP nanoparticles.[37] Thus, the impact of template on particle size seems to largely depend on the polarity of template and the strength of its molecular interaction with the functional monomer.

Binding properties of propranolol-imprinted nanoparticles

To evaluate the binding properties of nanoparticles, batch mode radioligand binding experiments were carried out. As shown in Figure 4, NIP1 and NIP2 bind less than 10% of [^{3}H]-labeled propranolol even at the highest particle concentration (2.0 mg mL^{-1}). NIP3, which has a higher MAA content, shows higher binding for [^{3}H]-labeled propranolol. On the other hand, propranolol binding with all the MIP nanoparticles is significantly higher than with the corresponding NIP nanoparticles, indicating the successful formation of the template-directed binding sites. It should be pointed out that the binding capability of MIP particles is not determined by the

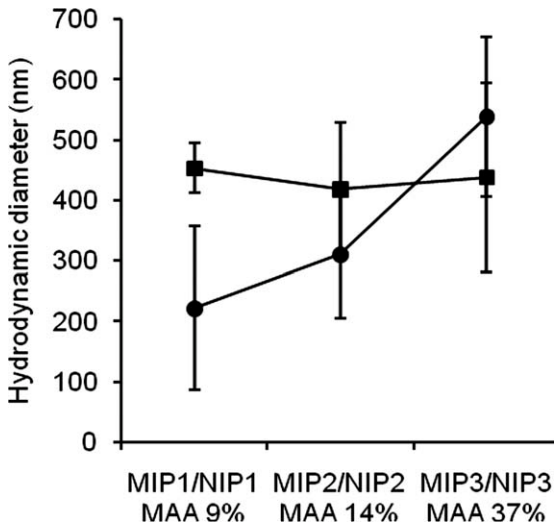

Figure 3 Summary of particle size distribution of nanoparticles determined by dynamic light scattering (DLS). (a) MIPs (circle) and (b) NIPs (square).

MAA content alone. Among the three imprinted polymers, MIP2 displays the highest propranolol binding, and the amount of MIP2 required to bind 50% of [^{3}H]-labeled propranolol ($C_{50\%}$) is as low as 0.7 mg mL^{-1}. At this polymer concentration, the total amount of propranolol bound by MIP2 is $\sim$ 176 fmol/mg polymer. Meanwhile, the amount of nonspecific binding to polymer matrix can be roughly estimated to be 6 fmol/mg polymer, from the amount of propranolol bound by the corresponding nonimprinted nanoparticles (NIP2). Herein, by subtracting the amount of the nonspecific binding, the amount of the high affinity binding sites on MIP2, at equilibrium, can be estimated to be $\sim$ 170 fmol/mg polymer, which is more than 20 times greater than the amount of nonspecific binding. Binding capability of MIP1 is slightly lower than that of MIP2; however, the steep increase of its binding curve in the low polymer concentration range, as shown in Figure 4, suggests that high affinity binding sites exist in both MIP1 and MIP2. In contrast, the $C_{50\%}$ of MIP3 is out of the tested polymer concentration range, suggesting that propranolol binding of this polymer is lower than that of MIP1 and MIP2. From the results, two additional important conclusions can be drawn: (3) The NIPs exhibit a limited nonspecific binding, which is apparently in proportion to the amount of MAA units incorporated in the particles. (4) Whereas a low MAA content results in a loss of binding capability, a high MAA/TRIM ratio combined with low crosslinking density also has the same effect, presumably due to the reduced rigidity of the polymer matrix that is unable to maintain the fidelity of the imprinted sites.[20,38,39]

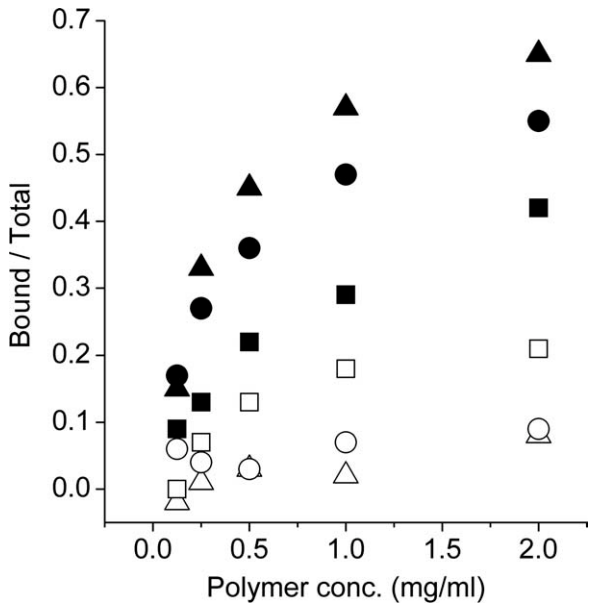

Figure 4 Uptake of [^{3}H]-(S)-propranolol (246 pM) in citrate buffer (25 m*M*, pH 6.0): acetonitrile (50 : 50, v/v) with increasing amount of imprinted and non-imprinted control polymer beads: (a) MIP1: MAA 9 wt % (filled circle), (b) MIP2: MAA 14 wt % (filled triangle), (c) MIP3: MAA 37 wt % (filled square), (d) NIP1: MAA 9 wt % (open circle), (e) NIP2: MAA 14 wt % (open triangle), and (f) NIP3: MAA 37 wt % (open square).

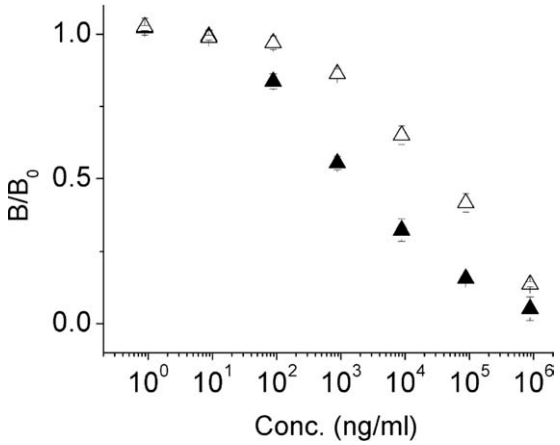

Figure 5 Displacement of [^{3}H]-(S)-propranolol (246 pM) binding to 0.5 mg of MIP2 in citrate buffer (25 m*M*, pH 6.0): acetonitrile (50 : 50, v/v) with increasing amount of (S)-propranolol (filled triangle) and (R)-propranolol (open triangle). Data were mean value $\pm$ standard deviation (n = 3). B/B0 is the ratio of the amount of [3H]-(S)-propranolol bound in the presence of displacing ligand, *B*, to the amount bound in the absence of displacing ligand, *B*0.

Finally, the specificity of the binding sites was investigated by studying the displacement of [^{3}H]-(*S*)-propranolol from the imprinted nanoparticles MIP2 with unlabeled (*R*)- and (*S*)-propranolol (Fig. 5). As shown, (*S*)-propranolol displaces more efficiently [^{3}H]-(*S*)-propranolol than (*R*)-propranolol. The cross-reactivity of the (*S*)-propranolol-imprinted sites toward (*R*)-propranolol, as represented by the ratio of IC_{50} values of (*S*)- and (*R*)-propranolol, was about 5%. This indicates that MIP2 has well-defined binding sites as a result of the successful molecular imprinting process.

CONCLUSIONS

In this study, the influences of template/functional monomer/crosslinking monomer ratios on the size and binding properties of propranolol-imprinted nanoparticles have been investigated. In all the cases, the functional monomer/crosslinking monomer ratio influences the binding capability of the nanoparticles. Interestingly, this ratio does not affect significantly the size of the obtained nanoparticles unless the template is added in the prepolymerization mixture. In addition, the template/functional monomer ratio turned out to be a critical factor influencing the final particle size. The rigidity of the polymer matrix was found to be important to achieve MIPs with high binding capability. Our results show that it is possible to

adjust both physical size and template binding capability of MIP nanoparticles by simply varying the ratio of template/functional monomer/crosslinking monomer in precipitation polymerization systems. Besides offering molecular selective adsorbents, the versatility of tuning nanoparticle characteristics (e.g., particle size) using extrinsic small molecules is interesting and may open new opportunities for a variety of clean polymer nanoparticles that can be conveniently synthesized by precipitation polymerization.

References

1. Arshady, R. Colloid Polym Sci 1992, 270, 717.
2. Asua, J. M. J Polym Sci Part A: Polym Chem 2004, 42, 1024.
3. Antonietti, M.; Landfester, K. Prog Polym Sci 2002, 27, 689.
4. Sherrington, D. C. Chem Commun 1998, 2275.
5. Xia, Y. N.; Gates, B.; Yin, Y. D.; Lu, Y. Adv Mater 2000, 12, 689.
6. Katz, E.; Willner, I. Angew Chem Int Ed 2004, 43, 6042.
7. Gao, X.; Yang, L.; Petros, J. A.; Marshall, F. F.; Simons, J. W.; Nie, S. Curr Opin Biotech 2005, 16, 63.
8. Ito, A.; Shinkai, M.; Honda, H.; Kobayashi, T. J Biosci Bioeng 2005, 100, 1.
9. Neuberger, T.; Schöpf, B.; Hofmann, H.; Hofmann, M.; von Rechenberg, B. J Magn Magn Mater 2005, 293, 483.
10. Wulff, G. Chem Rev 2002, 102, 1.
11. Haupt, K.; Mosbach, K. Chem Rev 2000, 100, 2495.
12. Hoshino, Y.; Kodama, T.; Okahata, Y.; Shea, K. J. J Am Chem Soc 2010, 130, 15242.
13. Ye, L.; Mosbach, K. Chem Mater 2008, 20, 859.
14. Poma, A.; Turner, A. P.; Piletsky, S. A. Trends Biotechnol 2010, 12, 629.
15. Svenson, J; Nicholls, I. A. Anal Chim Acta 2001, 435, 19.
16. Vlatakis, G.; Andersson, L. I.; Müller, R.; Mosbach, K. Nature 1993, 361, 645.
17. Andersson, L. I.; Müller, R.; Vlatakis, G.; Mosbach, K. Proc Natl Acad Sci USA 1995, 92, 4788.
18. Tse Sum Bui, B.; Haupt, K. Anal Bioanal Chem 2010, 398, 2481.
19. Ye, L.; Cormack, P. A. G.; Mosbach, K. Anal Commun 1999, 36, 35.
20. Ye, L.; Weiss, R.; Mosbach, K. Macromolecules 2000, 33, 8239.
21. Yoshimatsu, K.; Reimhult, K.; Krozer, A.; Mosbach, K.; Sode, K.; Ye, L. Anal Chim Acta 2007, 584, 112.
22. Downey, J. S.; McIsaac, G.; Frank, R. S.; Stöver, H. D. H. Macromolecules 2001, 34, 4534.
23. Ye, L.; Yilmaz, E. In Molecularly Imprinted Materials: Science and Technology; Yan, M.; Ramström, O., Eds.; Marcel Dekker: New York, 2005, p 435.
24. Tamayo, F. G.; Casillas, J. L.; Martin-Esteban, A Anal Chim Acta 2003, 482, 165.
25. Jiang, M.; Zhang, J. H.; Mei, S. R.; Shi, Y.; Zou, L. J.; Zhu, Y. X.; Dai, K.; Lu, B. J Chromatogr A 2006, 1110, 27.
26. Wang, J. F.; Cormack, P. A. G.; Sherrington, D. C.; Khoshdel, E. Angew Chem Int Ed 2003, 42, 5336.
27. Schweitz, L.; Spegel, P.; Nilsson, S. Analyst 2000, 125, 1899.
28. Spegel, P.; Schweitz, L.; Nilsson, S. Electrophoresis 2001, 22, 3833.
29. de Boer, T.; Mol, R.; de Zeeuw, R. A.; de Jong, G. J.; Sherrington, D. C.; Cormack, P. A. G.; Ensing, K. Electrophoresis 2002, 23, 1296.
30. Castell, O. K.; Allender, C. J.; Barrow, D. A. Biosens Bioelectron 2006, 22, 526.
31. Ho, K. C.; Yeh, W. M.; Tung, T. S.; Liao, J. Y. Anal Chim Acta 2005, 542, 90.
32. Reimhult, K.; Yoshimatsu, K.; Risveden, K.; Chen, S.; Ye, L.; Krozer, A. Biosens Bioelectron 2008, 23, 1908.
33. Yoshimatsu, K.; Ye, L.; Lindberg, J.; Chronakis, S. Biosens Bioelectron 2008, 23, 1208.
34. Yoshimatsu, K.; Ye, L.; Stenlund, P.; Chronakis, I. S. Chem Commun 2022 2008, 17.
35. Yoshimatsu, K.; LeJeune, J.; Spivak, D. A.; Ye, L. Analyst 2009, 134, 719.
36. Li, K.; Stöver, H. D. H. J Polym Sci Part A: Polym Chem 1993, 31, 3257.
37. Long, Y.; Philip, J. Y.; Schillén, K.; Liu, F.; Ye, L. J Mol Recognit 2011, 24, 619.
38. Wulff, G.; Kemmerer, R.; Vietmeier, J.; Poll, H. G. Nouv J Chim 1982, 6, 681.
39. Sellergren, B. Macromol Chem Phys 1989, 190, 2703.